Journal of Bacteriology

Coevolution of ABC Transporters and Two-Component Regulatory Systems as Resistance Modules against Antimicrobial Peptides in Firmicutes Bacteria

Sebastian Dintner, Anna Staron, Evi Berchtold, Tobias Petri, Thorsten Mascher and Susanne Gebhard

J. Bacteriol. **2011, 193(15):3851. DOI: 10.1128/JB.05175-11. Published Ahead of Print 10 June 2011.**

JOURNAL OF BACTERIOLOGY, Aug. 2011, p. 3851–3862 Vol. 193, No. 15
0021-9193/11/$12.00 doi:10.1128/JB.05175-11

Coevolution of ABC Transporters and Two-Component Regulatory Systems as Resistance Modules against Antimicrobial Peptides in *Firmicutes* Bacteria▽†

Sebastian Dintner,[1]§ Anna Staroń,[1]§ Evi Berchtold,[2] Tobias Petri,[2] Thorsten Mascher,[1] and Susanne Gebhard[1]*

Department of Biology I, Microbiology, Ludwig-Maximilians-Universität München, Planegg-Martinsried, Germany,[1] and Department of Informatics, Research and Teaching Unit Bioinformatics, Ludwig-Maximilians-Universität München, Munich, Germany[2]

Received 27 April 2011/Accepted 27 May 2011

In *Firmicutes* bacteria, ATP-binding cassette (ABC) transporters have been recognized as important resistance determinants against antimicrobial peptides. Together with neighboring two-component systems (TCSs), which regulate their expression, they form specific detoxification modules. Both the transport permease and sensor kinase components show unusual domain architecture: the permeases contain a large extracellular domain, while the sensor kinases lack an obvious input domain. One of the best-characterized examples is the bacitracin resistance module BceRS-BceAB of *Bacillus subtilis*. Strikingly, in this system, the ABC transporter and TCS have an absolute mutual requirement for each other in both sensing of and resistance to bacitracin, suggesting a novel mode of signal transduction in which the transporter constitutes the actual sensor. We identified over 250 such BceAB-like ABC transporters in the current databases. They occurred almost exclusively in *Firmicutes* bacteria, and 80% of the transporters were associated with a BceRS-like TCS. Phylogenetic analyses of the permease and sensor kinase components revealed a tight evolutionary correlation. Our findings suggest a direct regulatory interaction between the ABC transporters and TCSs, mediating communication between both components. Based on their observed coclustering and conservation of response regulator binding sites, we could identify putative corresponding two-component systems for transporters lacking a regulatory system in their immediate neighborhood. Taken together, our results show that these types of ABC transporters and TCSs have coevolved to form self-sufficient detoxification modules against antimicrobial peptides, widely distributed among *Firmicutes* bacteria.

In an era in which resistance against antibiotic compounds is becoming a major health issue worldwide, much attention is being given to the development of new drugs. In recent years, antibiotics that target the lipid II cycle of bacterial cell wall synthesis have been promoted as promising candidates. This group of compounds includes, for example, the glycopeptide vancomycin, lipodepsipeptides like ramoplanin, the cyclic peptide bacitracin, and most members of the large class of lantibiotics (9). The latter two are produced mainly by low-G+C Gram-positive microorganisms (*Firmicutes*) and target closely related species (27, 29).

As with most antibiotics, resistance against antimicrobial peptides has been observed, and the major mechanism appears to be via alterations of cell envelope charge and composition (9, 13). Additionally, producer self-resistance against lantibiotics is often mediated by ATP-binding cassette (ABC) transporters, collectively termed LanFEG, consisting of two membrane-spanning subunits and one ATPase, which are encoded in the biosynthetic loci for the respective lantibiotic and whose expression is regulated by a two-component system (TCS) of the same genetic locus (21). Over the last decade, several ABC transporters of a different type have been identified as resistance determinants against peptide antibiotics in nonproducing strains (5, 12, 32, 35, 39, 41, 44, 51). The permeases of these transporters share unique domain architecture with 10 transmembrane helices and a large extracellular domain (ECD) of about 200 amino acids between helices 7 and 8. They have been classified as the peptide-7 exporter (Pep7E) family in the Transport Classification Database (TCDB) (47). Regulation of these transporters generally also occurs via TCSs, which are most commonly encoded in an operon adjacent to that of the transporter (12, 31, 34, 39, 40, 42). The histidine kinases (HKs) of these TCSs belong to the intramembrane-sensing histidine kinase (IM-HK) group and are characterized by the possession of two transmembrane helices with a short (2- to 10-amino-acid) extracellular linker and no cytoplasmic domains besides the DHp (dimerization histidine phosphotransfer [23], also referred to as the H-kinase_dim domain in the Pfam database) and catalytic domains (37). An apparent widespread cooccurrence of these types of transporters and regulatory systems among the *Firmicutes* bacteria was noted as early as 2002 (30), and this study was recently updated by the same group (14).

One of the best-understood examples of this resistance mechanism is the BceRS-BceAB module of *Bacillus subtilis* (Fig. 1), which confers resistance against bacitracin, actagardine, and mersacidin (38, 40, 48). A striking characteristic of this system is the absolute requirement for the ABC trans-

* Corresponding author. Mailing address: Ludwig-Maximilians-Universität München, Department of Biology I, Microbiology, Grosshaderner Str. 2-4, D-82152 Planegg-Martinsried, Germany. Phone: 49 (0) 89-2180-74659. Fax: 49 (0) 89-2180-74626. E-mail: susanne.gebhard@bio.lmu.de.

§ Both authors contributed equally to this work.

† Supplemental material for this article may be found at http://jb.asm.org/.

▽ Published ahead of print on 10 June 2011.

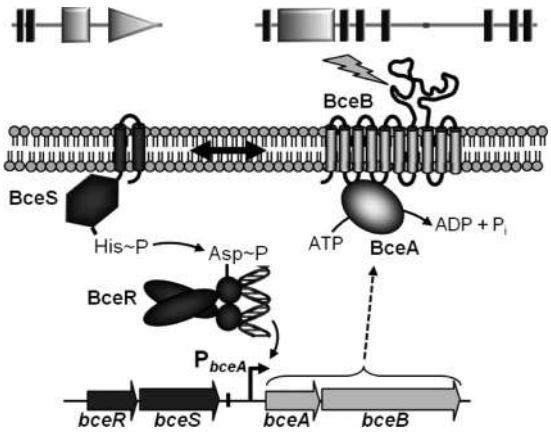

FIG. 1. Schematic diagram of the BceRS-BceAB bacitracin resistance module of *Bacillus subtilis*. Names of relevant proteins and genes are given. The presence of antimicrobial peptides is indicated by a lightning bolt. The proposed interaction between BceB and BceS is shown by a double-headed arrow. The phospho-relay between BceS and BceR, ATP hydrolysis by BceA, and activation of the *bceA* promoter (P_{bceA}) by BceR are shown by single-headed arrows, and increased expression of *bceAB* is shown by a dashed arrow (diagram adapted from reference 46). The domain architectures of BceS and BceB, as predicted by the SMART database (33), are indicated above. Transmembrane domains are depicted as black rectangles, the DHp and catalytic domains of BceS are shown as a shaded square and triangle, respectively, and the FtsX domain of BceB is shown as a shaded rectangle.

porter (BceAB) for bacitracin-dependent induction of *bceAB* expression, showing that the HK (BceS) alone is unable to detect the presence of the antimicrobial peptide (7, 46). The current working model assumes the existence of a sensory complex between the transporter and TCS. Furthermore, it has also been shown that the presence of the permease's ECD was indispensable for signaling, leading to the proposition that this region might constitute the substrate recognition domain of the module (46). Requirement of the ABC transporter for signal transduction was also observed in the bacitracin resistance module MbrABCD of *Streptococcus mutans* (42), and regulation of the vancomycin resistance transporter VraFG of *Staphylococcus aureus* appears to involve at least the permease component VraG (39). Taken together with their conserved genomic cooccurrence, these findings suggest that a regulatory interplay between the ABC transporter and TCS is a common theme in these antimicrobial peptide resistance modules.

To address this hypothesis, we carried out a comprehensive phylogenetic study and coclustering analysis of these systems and identified a clear coevolutionary relationship between transport permeases and HKs. Additionally, we closely investigated the ECDs with regard to their primary sequences and secondary structures, and we identified conserved putative response regulator binding sites in the promoter regions of the transporter operons. Furthermore, based on the observed coclustering of HKs and transport permeases, we could identify putative corresponding TCSs for transporters lacking regulatory systems in their immediate neighborhood. Our findings suggest the existence of a sensory complex between transporter and HK and thus a novel signaling mechanism involved in the resistance of *Firmicutes* bacteria against peptide antibiotics.

MATERIALS AND METHODS

Data acquisition. An initial data set was generated based on homology to BceRSAB (40), PsdRS-AB (48), and YxdJK-LM (31) of *B. subtilis* by performing a BLASTP search (1) with default parameters (scoring parameters matrix, BLOSUM62; gap opening penalty, 11; gap extension penalty, 1) of all microbial genomes available in the NCBI database as of April 2009, using each of the 12 protein sequences as a query. Of each result list, the top 250 hits were chosen and sorted to match HK, response regulator, ATPase, and permease components belonging to the same genetic locus. After removal of duplicates, 185 systems were obtained. Because we found BceB-like permeases to contain a PFAM FtsX domain, located in the region encompassing transmembrane helices 2 to 4 (Fig. 1), a second search was conducted by querying the SMART 6 database (33) for proteins containing such a domain. Of the 4,492 hits obtained, 274 were found to possess the typical transmembrane architecture of BceB-like proteins, containing 10 transmembrane helices with a large loop of approximately 200 amino acids between helices 7 and 8. These proteins were added to our original data set with removal of duplicates, resulting in a total number of 266 systems. In the Archaeal and Bacterial ABC Systems Database (ABCdb; January 2010 version) (http://www-abcdb.biotoul.fr), BceB-like permeases belong to subfamily M_9. We therefore searched this subfamily for proteins with greater than nine predicted transmembrane sections. The resulting 114 hits were checked for the BceB-like domain architecture, but no sequences not already contained in our data set were found. Additionally, the TCDB (47) was searched for Pep7E family transporters, but again, no new BceB-like sequences were identified in this database. Final refinement of our data set was carried out by analyzing the genomic neighborhood of all obtained sequences for genes with similarity to response regulators, ATPases, and HKs using the MicrobesOnline database (18). HKs and their corresponding response regulators were included only if the kinase showed the same domain architecture as BceS of two transmembrane helices separated by approximately 2 to 10 amino acids. The resulting data set is shown in Table S1 in the supplemental material.

Phylogenetic analyses. Multiple sequence alignments of permeases and HKs were obtained with ClustalW2 (50) using the Gonnet280 substitution matrix and default parameters (gap opening penalty, 10; gap extension penalty, 0.2; gap distance penalty, 5) at the European Bioinformatics Institute website (http://www.ebi.ac.uk). The resulting alignments were manually edited to remove gaps in order to allow calculation of meaningful phylogenetic trees (4). In particular, the region containing the ECD of the permeases, corresponding to positions 310 to 520 in *B. subtilis* BceB, was deleted from the alignment followed by realignment of the remaining sequence, because of the very poor conservation observed in this region. Phylogenetic trees were constructed from both of the sequence alignments with the neighbor-joining method implemented in BioNJ (25), using the Dayhoff PAM substitution matrix, 100 bootstraps, and otherwise default parameters on the Phylogeny.fr website (19). Graphical editing of the phylogenetic trees to allow direct comparison by a mirror-image display was performed in TreeDyn 198.3 (10).

Analysis of coevolution. Coevolving protein families undergo simultaneous sequence changes or conservation (26). In addition to our data set of BceRS-BceAB-like modules (see Table S1 in the supplemental material), we compiled two new data sets to use as controls (i.e., not coevolving proteins). For this, we analyzed the genomes represented in our original data set for a HK and a transport permease that were present in a large number of species but were not functionally associated with each other. These criteria were fulfilled by homologs of the HK YycG of *B. subtilis* and those of the permease OppB of *B. subtilis*. A total of 26 of the 96 different species represented in our data set were found to contain homologs to both of the proteins (see Table S2 in the supplemental material). For further analyses, we used the six obtained sequence families (BceR, BceS, BceA, BceB, YycG, and OppB) in data sets of 26 ("core") and 180 ("extended"; only for Bce homologs) sequences. For each data set, a multiple sequence alignment of all sequences ("complete") was generated using ClustalW2 as described above, consisting of 26 (core set) or 180 (extended set) sequences. Additionally, 50 randomly chosen subsets of 20 sequences were extracted from each core or extended set ("sampled") and realigned.

The sampled subset comparisons estimate alignment stability in terms of single sequence effects. Pairwise calculation of alignment correlations, using either complete or sampled alignments, was then carried out as follows. For a family, k, containing the sequences $s_i \in S^k$, $i = 1 \ldots |S^k|$, the comparison was done by computing a matrix, M, of normalized pairwise sequence identities (*id*) as follows: $\boldsymbol{M}^k = (m^k)_{ij}$, $i, j \in \{1 \ldots |S^k|\}$, where $m^k_{ij} = id(s_i, s_j)/0.5 \times (|s_i| + |s_j|)$, $s_i, s_j \in S^k$, $s_i \neq s_j$. Two matrices for families k and l were then compared using the linear correlation coefficient (CC), as introduced by Goh and coworkers (26):

$$CC = \frac{\sum_{i=1}^{|n|-1}\sum_{j=i+1}^{|n|}(M_{ij}^{k} - \overline{M^{k}})(M_{ij}^{l} - \overline{M^{l}})}{\sqrt{\sum_{i=1}^{|n|-1}\sum_{j=i+1}^{|n|}(M_{ij}^{k} - \overline{M^{k}})^2}\sqrt{\sum_{i=1}^{|n|-1}\sum_{j=i+1}^{|n|}(M_{ij}^{l} - \overline{M^{l}})^2}}$$

To assess the significance of the CC for the pair of BceB-like and BceS-like sequences, we used all pairs containing OppB and/or YycG as negative controls and the pairs of BceA-BceB, BceS-BceR as positive controls, computing both core and sampled comparisons. The results served as background distributions of known noninteracting and interacting protein families.

Secondary structure prediction of the large extracellular domain of transport permeases. For a detailed analysis of the ECD of the permeases, the region corresponding to positions 310 to 520 of *B. subtilis* BceB, which had previously been removed from the sequence alignments, was extracted from all sequences. The obtained sequences were sorted into eight sets according to the classification of permeases described in this study. From each group, a representative set was chosen. For this, pairwise identities were calculated for all sequence pairs, and from each cluster sharing over 80% identity, only one randomly chosen sequence was included in further analyses. Multiple sequence alignments for each of the eight sets were generated with ClustalW2 as described above. Additionally, the secondary structure was predicted for several sequences in each set using JPred3 (11), and the results were integrated into the sequence alignment. A consensus secondary structure for each of the eight groups was deduced from these alignments.

Identification of response regulator binding sites. Upstream regions of operons encoding Pep7E ABC transporters were retrieved from the MicrobesOnline database (18). Generally, 250 nucleotides (nt) upstream of the start codons were analyzed, unless the distance to the nearest upstream gene was greater than 250 nt. In this case, the whole intergenic region was analyzed. If the gene encoding the ATPase subunit was not the first in the predicted operon, both 250 nt upstream of the ATPase gene and the region upstream of the preceding gene were analyzed. Retrieved sequences were subjected to conserved motif searches using MEME (3) (http://meme.sdsc.edu/) with the following parameters: distribution, any number of repetitions; width, minimum of 5, maximum of 20. Analysis with MEME was followed by in-depth manual analysis. Sequence motifs were illustrated based on a position weight matrix using the WebLogo tool (15) (http://weblogo.berkeley.edu).

RESULTS

Genomic arrangement and phyletic distribution of Pep7E transporters and TCSs. Based on sequence similarity to the three previously described resistance modules of *B. subtilis* (BceRS-AB, PsdRS-AB, and YxdJK-LM) and on the typical domain architecture of Pep7E permeases (ten transmembrane helices, large ECD between helices 7 and 8, FtsX domain encompassing helices 2 to 4) (Fig. 1), we identified a total of 266 BceAB-like ABC transporters, as described in Materials and Methods (see Table S1 in the supplemental material). Next, we analyzed the genomic context of all permeases in our data set for response regulators, HKs, and ATPases. TCSs were included only if their HK possessed the typical domain architecture of BceS-like IM-HK (37) (Fig. 1). Of the total of 266 permeases, we found 22 orphan permeases lacking an ATPase (Table 1). However, 14 of these were found in the immediate neighborhood of a second, complete Pep7E transporter as discussed below. Moreover, 181 BceS-like HKs were identified (Table 1). In total, 213 (80%) of the transporters in our data set were associated with a BceRS-like TCS (Fig. 2A; see also Table S1 in the supplemental material). All further analyses reported in this study were restricted to the permease and HK components of the modules, which are here referred to as BceB-like and BceS-like, respectively. Beyond the genes described here, no conservation of a genomic context was found for these modules. However, in a few cases, additional genes with a putative role in resistance against cell wall active antibiotics were carried in the same locus, such as undecaprenyl pyrophosphate phosphatase (*uppP*)-like genes in four clostridial species and a *vanZ*-like gene in the Ysa locus of *Lactococcus lactis* (not shown). UppP-like proteins are involved in bacitracin resistance (6), and VanZ of *Enterococcus faecium* confers resistance to teicoplanin, a glycopeptide antibiotic also interfering with the lipid II cycle of cell wall synthesis (2).

TABLE 1. Phyletic distribution and cooccurrence of ABC transporters with TCSs

Order	Phylum	No. of:		
		ABC transporters[a]		Associated TCSs[b]
		Complete	Orphan permease	
Bacillales	*Firmicutes*	116	20	87
Lactobacillales		34		16
Clostridiales		87	2	71
Erysipelotrichales		2		2
Thermoanearobacterales		1		1
Coriobacteriales	*Actinobacteria*	2		2
Spirochaetales	*Spirochaetes*	1		1
Unclassified	Unclassified	1		1
Total		244	22	181

[a] Transporters listed as "complete" are encoded by adjacent genes for the ATPase and permease, and transporters listed as "orphan permease" are those for which no ATPase gene was found immediately adjacent to the permease gene.

[b] TCSs listed as "associated" were found in the same genetic locus (within a six-gene distance) as a transport permease.

Among our data set, 10 systems had been described previously (Fig. 2A and Table 2). The common trait of all these systems was their involvement in resistance against antimicrobial peptides, suggesting that the function of Pep7E transporters is restricted to the detoxification of peptide antibiotics. In good agreement with other studies (14, 30), nearly all modules in our data set were found in the phylum *Firmicutes*. The vast majority (97%) of these were distributed among the orders *Bacillales*, *Clostridiales*, and *Lactobacillales* (Table 1). Only four systems were found in other bacterial phyla: two in the *Actinobacteria*, one in a spirochete, and one in an unclassified bacterium. Most members of the *Lactobacillales* contained only one (e.g., *Streptococcus mutans*) or two (e.g., *Lactobacillus rhamnosus*) copies of such resistance modules. In contrast, members of the *Bacillales* and *Clostridiales* usually contained several copies and, in some cases, up to six modules (e.g., *Bacillus cereus* and *Clostridium sporogenes*) (see Table S1 in the supplemental material).

Phylogenetic analysis of the permease and HK components. To analyze the phylogenetic relationship of the transport permeases and HKs, we first created multiple sequence alignments with ClustalW2 (50). Both sets of proteins showed good sequence conservation across the data set, with the permeases sharing 25% to 40% pairwise sequence identity and the HKs sharing 20% to 55% pairwise sequence identity at the amino acid level. Notably, the region of the permeases containing the large ECD (corresponding to positions 310 to 520 in *B. subtilis* BceB) showed only very low sequence similarity, with less than 10% pairwise sequence identity observed, resulting in a poor alignment across this region (not shown). We therefore excluded the entire ECD from the phylogenetic analysis. A phylogenetic tree of the transport permeases calculated by the

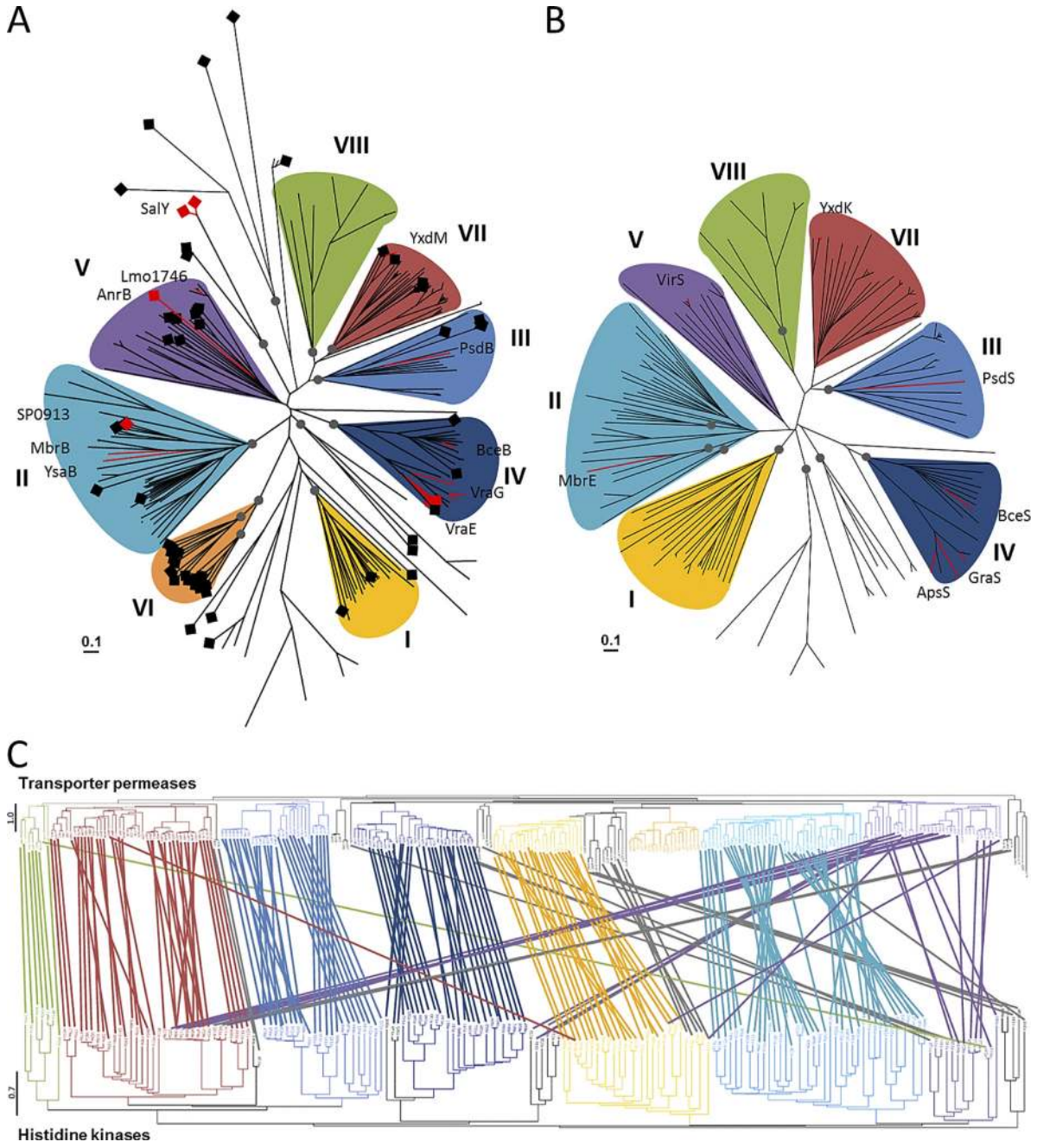

FIG. 2. Phylogenetic trees and coevolution of Pep7E-type permeases and BceS-like HKs. Phylogenetic trees were calculated by the neighbor-joining (NJ) method for both protein families. (A and B) Lines for previously described systems are shown in red, and names of corresponding proteins are given. (A) NJ tree of transport permeases. Permeases lacking a neighboring TCS are marked with black or red squares. The assignment of the eight phylogenetic groups (I to VIII) is shown by different colors. (B) NJ tree of HKs. Assignment of phylogenetic groups is color coded to match the corresponding groups shown in panel A. (C) Mirror-image display of the NJ trees of permeases (top) and HKs (bottom). Color coding was done as described for panels A and B. Lines were drawn from each permease to the HK encoded in the same locus, using the color indicating the permease's group assignment. Scale bars show the number of expected amino acid replacements per site as calculated for each phylogenetic tree. Bootstrap values of above 0.5 for the central branches are indicated by gray dots (shown only in panels A and B).

neighbor-joining method showed eight distinct groups (Fig. 2A). Seven of these were supported by bootstrap values of above 0.5 (i.e., they occurred in over 50% of 100 random bootstrapping replicates) (Fig. 2A, gray dots). We labeled these groups I to VIII. A recently published grouping of this type of transporter reported six distinct phylogenetic groups (14). For reasons of consistency, we assigned the same group numbers where possible, which required splitting the previously assigned group III into our groups III, VII and VIII. We next calculated a neighbor-joining tree of the HKs, which showed the existence of seven distinct groups; however, only three of these were supported by bootstrap values of above 0.5

TABLE 2. In depth analysis of the phylogenetic groups

Group	No. of permeases	Genera[a]	No. of HKs[b]	Example permease(s)	Substrate (inducer) range[c]	Reference(s)
I	24	Clo (14), Bac (2), Eub (2), Ana (1), Ato (1), Bry (1), Col (1), Cop (1), Rum (1)	22 (22)			
II	43	Str (11), Clo (8), Rum (4), Lac (3), Sta (3), Bla (2), Des (2), Dor (2), Cal (1), Cat (1), Eub (1), Hol (1), Lac (1), Leu (1), Ros (1), Tre (1)	39 (38)	MbrB, SP0913, Spr0813, YsaB,	Bacitracin, gramicidin, lincomycin, nisin, vancoresmycin,	5, 32, 35, 42, 51
III	28	Bac (19), Clo (5), Pae (2), Sym (1), The (1)	22 (22)	PsdB	Enduracidin, gallidermin, nisin, subtilin, (actagardine)	48
IV	32	Sta (13), Bac (11), Geo (4), Alk (2), Lys (1), Oce (1)	26 (23)	BceB, VraE, VraG	Bacitracin, hBD3, indolicidin, LL-37, nisin, polymyxin B, vancomycin, actagardine, mersacidin	7, 34, 39, 44, 46, 48
V	37	Bac (13), Clo (13), Lis (8), Alk (2), Eub (1)	22 (8)	AnrB, Lmo1746	Bacitracin, β-lactam antibiotics, gallidermin, nisin	12, 36
VI	19	Bac (9), Lac (8), Ent (1), Ped (1)	0			
VII	44	Bac (34), Clo (4), Geo (4), Bre (1), Ent (1)	26 (25)	YxdL	(LL-37)	45
VIII	8	Bac (3), Clo (2), Alk (1), Ana (1), Lys (1)	8 (7)			

[a] Abbreviations: Alk, *Alkaliphilus*; Ana, *Anaerococcus*; Ato, *Atopobium*; Bac, *Bacillus*; Bry, *Bryantella*; Bre, *Brevibacillus*; Bla, *Blautia*; Cal, *Caldicellulosiruptor*; Cat, *Catenibacterium*; Cop, *Coprococcus*; Clo, *Clostridium*; Col, *Collinsella*; Des, *Desulfitobacterium*; Dor, *Dorea*; Ent, *Enterococcus*; Eub, *Eubacterium*; Geo, *Geobacillus*; Hol, *Holdemania*; Lis, *Listeria*; Lys, *Lysinibacillus*; Leu, *Leuconostoc*; Lac, *Lactococcus*; Oce, *Oceanobacillus*; Pae, *Paenibacillus*; Ped, *Pediococcus*; Sta, *Staphylococcus*; Sym, *Symbiobacterium*; Str, *Streptococcus*; The, *Thermobaculum*; Tre, *Treponema*; Ros, *Roseburia*; Rum, *Ruminococcus*. The number of systems from each genus is shown in parentheses.

[b] The number of HKs associated with transporters of this group. The number in parentheses shows the number of these HKs which belonged to the matching group in the phylogenetic tree of HKs.

[c] The substances given in parentheses are antimicrobial peptides, which were shown to induce expression of the transporter genes but against which the transporter did not confer resistance. It should be noted that the compounds listed as substrates may also act as inducers. hBD3, human β-defensin 3.

(Fig. 2B). Strikingly, there appeared to be a substantial similarity in the clustering of permeases and HKs belonging to the same genetic locus. To analyze this congruence more closely, we chose a layout in which both phylogenetic trees could be juxtaposed in a mirror-image display. Each permease was then linked to the HK from the same genetic locus by a line of the same color as that chosen to highlight its group assignment (Fig. 2C). From this, it was clear that, apart from a few exceptions (mainly permeases from group V associating with HKs from group VII) (Table 2), the HKs associated with permeases from one phylogenetic group also formed a distinct group in their own tree, suggesting a coevolution of both protein families (43). Curiously, no permease from group VI was associated with a TCS, which explained the presence of only seven HK groups rather than eight permease groups and is analyzed in more detail below.

Description and functional analysis of the phylogenetic groups. Following the division of transport permeases into the eight phylogenetic groups, we analyzed these groups for common traits or species distribution to see if it might be possible to assign putative functions to as-yet-uncharacterized systems. The details of this analysis are summarized in Table 2. While some groups, such as group II, were comprised of systems from a wide range of genera, others showed a more restricted species distribution, e.g., groups I, IV, VI, and VII. However, we could not detect the opposite correlation, i.e., modules from one species did not cluster into the same phylogenetic group. It was also not possible to detect any correlation between substrate range and phylogenetic group. Systems conferring bacitracin resistance were found in groups II, IV, and V, and those mediating nisin resistance were found in groups II, III, IV, and V (Table 2 and references therein).

A unique transport system in our data set was SalXY of *Streptococcus salivarius*, which could not be assigned to any of the eight groups (Fig. 2A). Regulation of this transporter is mediated by the TCS SalKR encoded downstream of *salXY* (53). However, the HK SalK did not show the typical BceS-like domain architecture and was therefore excluded from our data set. This deviation from the paradigm modules described in this study most likely reflects the fact that SalXY is the only system from our data set that is part of a biosynthetic locus for an antimicrobial peptide, salivaricin A, and is thought to mediate producer self-resistance (53).

Alignment correlation supports coevolution of TCSs and ABC transporters. A congruence of two phylogenetic trees, as we found for BceB-like permeases and BceS-like HKs, is generally taken to reflect a coevolution of both protein families (38). For example, the coevolution of HKs with their cognate response regulators was deduced from a qualitative comparison of their respective phylogenetic trees (26). While phylogenetic trees are useful for visual inspection, alignment correlations as introduced by Goh and colleagues (26) bypass the

ambiguous tree-building step and instead rely on similarity matrices computed directly from multiple alignments (see Materials and Methods). A correlation coefficient (CC) was, for example, calculated for chemokines and chemokine receptors to show the degree of similarity between the two trees (26). However, the interpretation of such results is somewhat problematic in that the similarity of phylogenetic trees of protein families is partly due to the underlying phylogeny of the species. Furthermore, additional effects can lead to an apparent coevolution of two proteins from the same organism, such as the fact that both of them are membrane localized, as is the case for the BceB- and BceS-like proteins. Usually, the significance of the obtained CCs is computed by shuffling the pairwise matrix row assignments, i.e., uncoupling the sequence pairs (26). But since such an approach removes all correlation effects on both protein and species levels, it will erroneously detect significant coevolution and therefore does not provide a sufficient control. A more accurate validation of the alignment correlation is to use selected interacting and noninteracting protein families as controls, which provide a direct and easy-to-interpret background.

As described in Materials and Methods, we analyzed the genomes from our data set for a HK and a transport permease that were present in a large number of species but were not functionally associated with each other. These criteria were fulfilled by the HK YycG (WalK), which is part of the essential YycFG (WalRK) TCS of the *Firmicutes* (22, 49), and the permease OppB, a component of the widely distributed oligopeptide importer OppABCDF (20). In combination with our data set of BceRS-BceAB homologs, all possible pairs of protein families involving a YycG and/or OppB homolog are assumed not to have coevolved, because there is no functional link between these proteins and Bce-like modules. As shown in Fig. 3, gray font, the CCs calculated for these pairs were in the range of approximately 0.4 to 0.6. This degree of correlation can thus be considered the background similarity when comparing any pairs of proteins from our selection of species. The second set of controls consisted of protein pairs known to physically interact, such as the two protein subunits of BceAB-like transporters or of BceRS-like TCSs, which can be assumed to have coevolved. Consistent with this, these pairs all showed high CC values of above 0.9 (Fig. 3A, gray shading). Importantly, the pair of proteins under investigation in the present study, i.e., homologs of BceB and BceS, displayed a similarly high CC of 0.97 (Fig. 3A, outlined), supporting our hypothesis of their coevolution. The remaining pairs also show high CC values, which is probably due to indirect effects, because they are all components of the same module (Fig. 3B), even if a direct interaction between, for example, the HK and the ATPase is unlikely.

To compensate for potential random effects introduced into the ortholog families by single sequences, we devised a subset sampling with subsequent realignment. Each multiple sequence alignment was thus split into 50 alignments of 20 sequences. Using these new alignments, 50 separate CCs were computed against each family. A box plot of the obtained results showed that, apart from a few outliers, all subsets of interacting pairs (positive controls and BceB-BceS pairs) showed CCs of above those calculated for noninteracting pairs, thus providing further validation of our approach (Fig. 3C).

A

	OppB	YycG	BceB	BceA	BceS
BceR	0.37	0.52	0.94 (0.78)	0.91 (0.91)	0.92 (0.84)
BceS	0.41	0.51	0.97 (0.82)	0.9 (0.72)	
BceA	0.43	0.62	0.93 (0.79)		
BceB	0.44	0.55			
YycG	0.64				

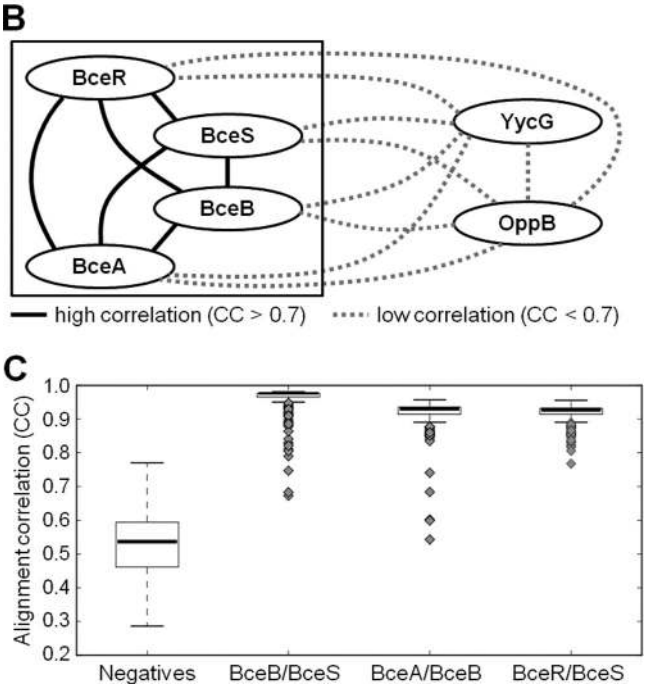

FIG. 3. Correlation coefficients and coevolved protein partners. (A) CCs calculated from complete core data sets ($n = 26$) for all combinations of protein family pairs. Results from extended sets ($n = 180$), where available, are given in parentheses. Values of negative-control pairs are shown in gray, and values of positive-control pairs are shown by gray shading. The field showing the CC of BceB-like permeases with BceS-like HKs is outlined in boldface. (B) Schematic presentation of correlation between all six protein families. Gray dotted lines show background correlation levels (CC < 0.7). Solid lines show correlation above the background (CC > 0.7). Components of Bce-like modules are boxed. (C) Box plot of randomly sampled CCs. Sequence subsets ($n = 20$) were extracted from core (negatives) or extended (all other pairs) data sets. In each column, 25% of values are lower than the bottom edge of the gray box (25% quartile), 50% are lower than the black line (median), and 75% are lower than the upper edge of the gray box (75% quartile). The whiskers show the most extreme data points within the 1.5-fold interquartile range; gray diamonds show data points outside this range. "Negatives" are all pairs involving at least one YycG or OppB homolog, and pairings of other protein families are given.

Taken together, these analyses showed that the degree of coevolution between BceB-like permeases and BceS-like HKs is as high as that between proteins known to physically interact and significantly higher than the background correlation caused by speciation effects.

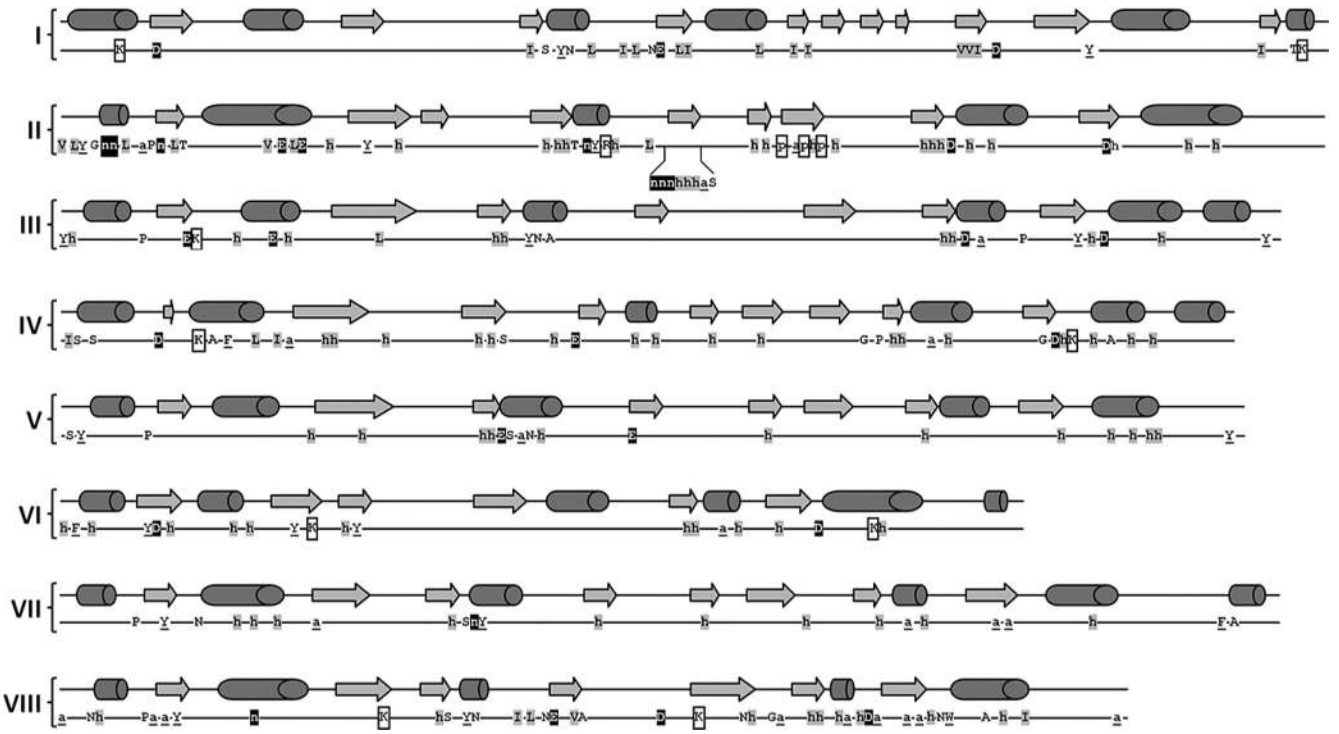

FIG. 4. Secondary structure and consensus motifs in the extracellular domains of transport permeases. For each of the phylogenetic groups (shown on the left), the consensus secondary structure, based on prediction by JPred3 (11) is displayed as α-helices (dark gray barrels) and β-sheets (light gray arrows). Conserved amino acids (threshold of 50%, based on analysis of ClustalW2 alignments in BioEdit [28]) are shown by one-letter codes on the bottom lines. Lowercase letters show conservation of amino acid type, as follows: h, hydrophobic (L, I, V, M); n, negative (D, E); p, positive (K, R); a, aromatic (Y, F). Hydrophobic (gray background), negatively charged (white letter on black background), positively charged (black box), or aromatic (underlined) residues are marked. Drawings are to scale for one representative sequence of each group (I, >106; II, >093; III, >070; IV, >069; V, >264; VI, >233; VII, >080; VIII, >053; [numbers given as GIs in the data set]). Complete alignments are shown in Fig. S1 in the supplemental material.

Primary and secondary structure analysis of the ECD. Our analysis of the phylogenetic groups described above could not identify any definite correlation between group assignment of a permease and its likely substrate range. While no information is available on the transport mechanism of Pep7E-type systems, the ECD of the permeases has been previously proposed to act as a substrate binding domain, based on its size and extracellular location (46). Sequence conservation of the ECD across the complete data set was poor, and thus, this region had been excluded from phylogenetic analyses. Following division of the permeases into the eight separate phylogenetic groups, we analyzed the ECD regions for group-specific characteristics, on the levels of both primary sequence and predicted secondary structure (see Fig. S1 in the supplemental material). The ECDs of the separate groups were similar in size, ranging from approximately 180 to 230 amino acids. Only group I possessed longer ECDs of 220 to 280 amino acids. Comparison of the secondary structures of all groups revealed a conserved arrangement of α-helices and β-sheets in the order α–β–α–$\beta_{2\text{-}3}$–α–$\beta_{3\text{-}4}$–α–β–$\alpha_{1\text{-}2}$, with only groups I and VI showing slight deviations (Fig. 4). We further identified individual conserved amino acid residues for each group (Fig. 4), although even within groups, sequence conservation of the ECDs was still moderate (Fig. S1). Conserved residues often appeared to cluster in the vicinity of the central α-helix and in the ultimate or penultimate β-sheet preceding the terminal α–β–$\alpha_{1\text{-}2}$ sequence. Mostly, the conservation applied to hydrophobic amino acids, but group II is characterized by a large number of both positively and negatively charged conserved residues, while groups VII and VIII contain several conserved aromatic side chains. Despite these findings, the sequence of the ECD again was not correlated with substrate range.

Binding sites for response regulators. For several BceRS-BceAB-like systems, a response regulator binding site has been identified in the promoter of the transporter operon (31, 36, 40, 42). The core consensus sequence appears to be an inverted repeat around a central ACA-N_4-TGT motif (17). Based on the assumption that the ABC transporters identified in the present study are generally regulated by their adjacent TCS, it should be possible to identify the response regulator binding sites in the promoter regions of the transporter operons. Moreover, the identification of multiple paralogous Bce-like modules from different groups in a single genome suggests sequence diversification in the regulator binding sites, which may be group specific, to ensure sufficient regulatory specificity and insulation. We therefore searched the upstream regions of each transport operon in our data set for sequences with similarity to the consensus motif mentioned above. In 70% of all promoter regions analyzed, a complete putative binding site was identified (see Table S3 in the supplemental material), and the overall consensus of these 186 sequences was found to be TNACA-N_4-TGTAA, with an AT-rich central 4-nt spacer (Fig. 5A). Next, we sorted the putative binding site sequences according to the eight phylogenetic groups and derived a con-

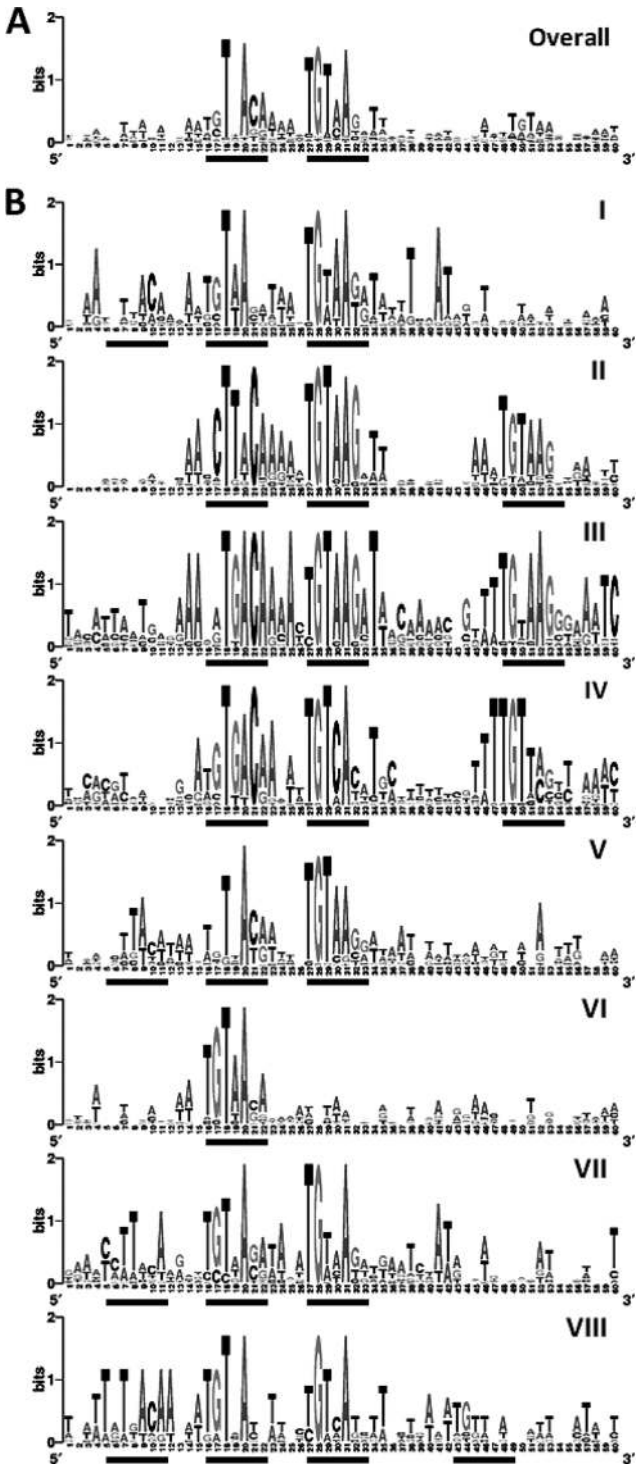

FIG. 5. Consensus sequences of putative response regulator binding sites in transport operon promoters. Regions 250 nt upstream of ATPase start codons were scanned for motifs with similarity to previously identified binding sites of BceR-like response regulators. (A) Overall consensus derived from all 192 identified putative binding sites. (B) Sequence logos showing the identified consensus sequences for each group separately (panels I to VIII). The seven nucleotide repeats are marked by black bars below each logo. Sequence logos were calculated by WebLogo (15), with 20 (group I), 39 (group II), 16 (group III), 31 (group IV), 29 (group V), 7 (group VI), 31 (group VII), or 8 (group VIII) putative binding sites identified.

sensus sequence for each group (Fig. 5B). The only group that perfectly matched the entire previously proposed consensus of ANCTTACA-N_4-TGTAAGNT (17) was group II. For most other groups, the best conserved positions appeared to be TGTNACA-N_4-TGTAAG, with a number of subtle differences between groups, as shown in Fig. 5B. Strikingly, in all but group VI, a third or even fourth repeat could be identified, located up- and/or downstream of the most highly conserved putative binding site, usually with a spacing of about 13 nt (Fig. 5B). A similar situation has been reported for the *mbrAB* operon of *S. mutans*, where this additional repeat did not appear to be required for DNA binding by the response regulator MbrC (42). Remarkably, in group VI, whose transporters lack a neighboring TCS, most promoters contained only half of a binding site, raising the question as to how expression of these systems may be regulated. Taken together, each group was found to possess a subtly unique binding consensus, further supporting the regulatory relationship between transporters and TCSs from matching phylogenetic groups.

Loci with multiple ABC transporters. As described above, we identified 20 loci in which a single TCS was located next to multiple transport permeases. These loci were analyzed in more detail by comparing the group assignments of the HK and all permeases to test if the coclustering also held true in such more complex gene arrangements. Furthermore, we scanned these regions for putative response regulator binding sites to identify likely regulated promoters. Schematic diagrams of each type of gene arrangement and group combination are shown in Fig. 6A. In *Bacillus* species, two main patterns were found. The first pattern is comprised of a group III TCS with several permeases from the same group. The second consists of a group VII TCS with multiple permeases from the same group and one or two transporters from group V. In other genera, the arrangements were more varied (Fig. 6A). Stretches of permeases from the same group often contained only a single ATPase gene, suggesting that either all permeases form complexes with the same ATPase or only one functional transporter is encoded. Another notable feature was the absence of any regulator binding sites upstream of permeases immediately following the TCS, which may indicate that these permeases are cotranscribed with the TCS and not regulated in response to a substrate antimicrobial peptide. In contrast, transporter operons divergently transcribed from the TCS always contained a binding site, but experimental evidence is needed to determine whether regulation occurs via the neighboring TCS.

Putative assignment of regulatory TCSs to orphan transporters. While the vast majority of ABC transporters identified in our study were encoded in a genetic locus together with a BceRS-like TCS, a number of transporters were lacking a neighboring TCS (Fig. 2A; see also Table S1 in the supplemental material). Based on the coclustering of permeases with HKs, we therefore next posed the question if it was possible to identify likely candidate HKs in the genomes, matching the classification of these orphan transporters. Of the genomes containing such systems, 25 were available in the Microbial Signal Transduction database MiST2 as of August 2010 (52). From these, the protein sequences of all HKs were retrieved. For each organism, the HKs were aligned with 15 representative sequences from our data set, and phylogenetic trees were

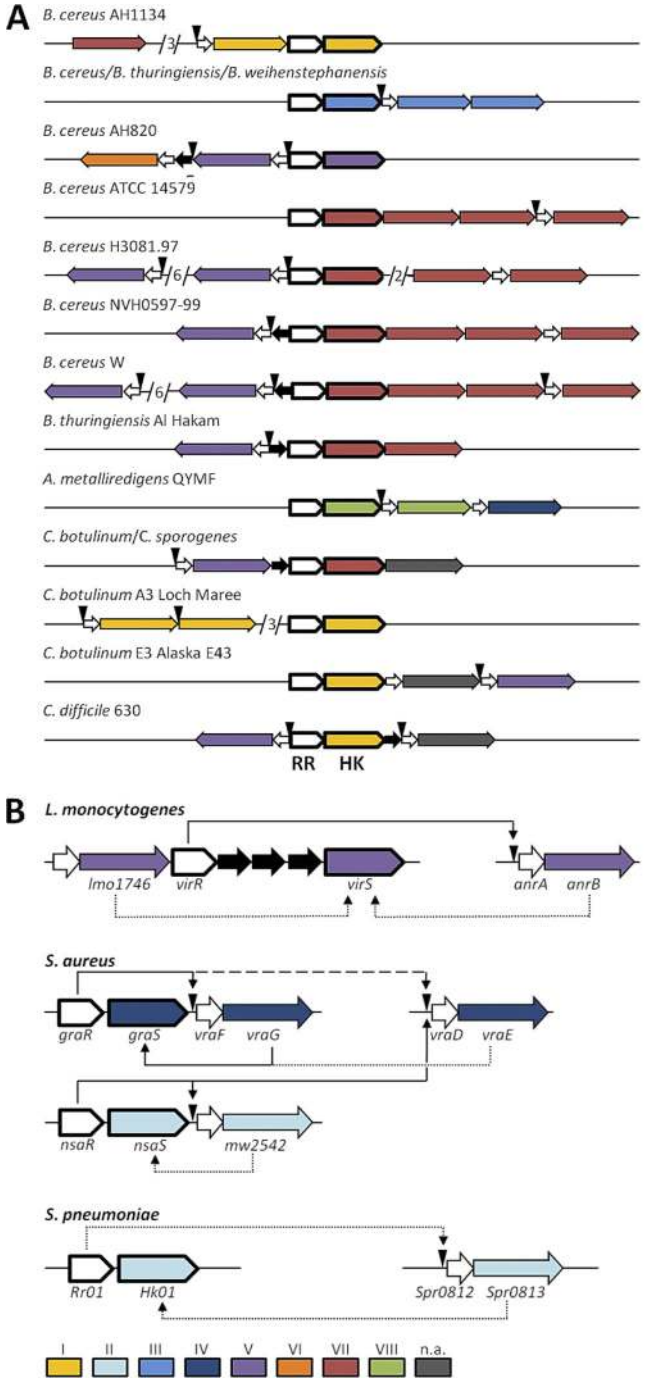

FIG. 6. (A) Schematic of genetic loci containing multiple transporter genes. The single TCS of each locus is shown in the center and marked by boldfaced contours. Response regulator (RR) and HK components are indicated. HKs and permease genes are colored according to their phylogenetic groups, as shown below. The ATPase genes are shown as small white arrows, and unrelated genes are shown as small black arrows. Where several unrelated genes were found in the gene locus, the line is broken and the number of intervening genes is indicated. Putative regulator binding sites are marked as black triangles. (B) Schematic of putative regulatory networks between separate genetic loci in example species. Markings of gene function, phylogenetic classification, and regulator binding sites are as described for panel A. Gene names or locus tags are shown. Experimentally proven regulation of promoters and interaction between transporters and HKs is indicated by solid arrows (corresponding references are given in the text). The partial regulation of *vraDE* expression by GraRS is indicated by a dashed line. Hypothetical regulatory interactions are indicated by dotted lines. Drawings not to scale. *B. cereus*, *Bacillus cereus*; *B. thuringiensis*, *Bacillus thuringiensis*; *B. weihenstephanensis*, *Bacillus weihenstephanensis*; *A. metalliredigens*, *Alkaliphilus metalliredigens*; *C. botulinum*, *Clostridium botulinum*; *C. difficile*, *Clostridium difficile*.

calculated using the PROTDIST and FITCH programs of the Phylip package implemented in BioEdit (24, 28). Kinases clustering in one branch with the BceS-like reference sequences were identified in eight of the genomes, with each of these genomes containing only a single such sequence.

To determine the group assignment of these newly identified HKs, their sequences were added to our data set and the phylogenetic tree was recalculated. Strikingly, for all eight new HKs, their group assignment matched that of the respective orphan transporter (Table 3), suggesting that they may indeed be responsible for the regulation of the transporter's expression. In eight of the genomes for which no new HK could be identified, a second BceAB-like transporter was present, which belonged to the same phylogenetic group as the orphan transporter and which possessed a matching TCS (Table 3). In these cases, it is conceivable that the TCS regulates the expression of both transporters. Thus, for a total of 15 orphan transporters, we could assign a putative regulatory system. Furthermore, in 12 of these, a potential regulator binding site was present in the promoter regions, supporting regulation by a BceRS-like TCS rather than by a different mode of gene regulation. Of the 15 systems for which no assignment of a putative regulatory TCS was possible, 12 belonged to group VI, and 8 of these did not contain a putative response regulator binding site in their promoter region. It is unclear if or how expression of this group of transporters is regulated.

DISCUSSION

In this study, we investigated the evolutionary and regulatory relationship between Pep7E-type ABC transporters and TCSs containing a BceS-like IM-HK, which together have been described as detoxification modules against peptide antibiotics (7, 39, 42, 46, 48). Our comprehensive data set generated from five independent database searches almost exclusively contained proteins from *Firmicutes* bacteria, and all previously described systems were involved in resistance against different antimicrobial peptides. Thus, it appears that these modules indeed evolved as a specific detoxification mechanism of *Firmicutes* bacteria against this class of drugs. Interestingly, the substrate compounds are also produced primarily by *Firmicutes* species and target species closely related to the producer organism (13, 27). It is therefore hardly surprising to find a phyletic distribution of the specific resistance genes similar to that of the ability for peptide antibiotic biosynthesis.

Phyletic distribution. The majority of the proteins were found in only three orders, the *Bacillales*, *Lactobacillales*, and *Clostridiales*. Whether this shows the true distribution of such resistance modules or rather reflects the strong bias in genome sequencing projects toward biotechnologically and medically relevant species (about 90% of all currently fully sequenced

TABLE 3. Assignment of a putative regulatory TCS to orphan transporters

Organism[e]	Permease		Binding site[c]	Histidine kinase	
	No. in data set[a]	Group[b]		GI or no. in data set[d]	Group[b]
A. metalliredigens	>224	V	−	>001	V
B. cereus	>272	VI	+	NM	
	>015	NA	−	NM	
	>220	VII	+	3002066	VII
B. thuringiensis	>222	VI	+	NM	
	>223	V	+	>076	V
	>226	VII	+	49477785	VII
E. faecalis	>255	VII	+	NM	
	>234	NA	−	29375511	NA
E. faecium	>258	VI	−	NM	
	>230	NA	−	69244814	NA
G. thermodenitrificans	>245	VII	+	−	
L. acidophilus	>233	VI	−	−	
L. brevis	>257	VI	−	−	
L. casei	>242	VI	−	NM	
L. delbrueckii	>251	VI	−	−	
L. gasseri	>235	VI	+	−	
L. johnsonii	>244	VI	+	−	
L. plantarum	>239	VI	−	−	
L. sakei	>259	VI	−	NM	
L. innocua	>264	V	+	>173	V
L. monocytogenes	>256	V	+	>174	V
L. welshimeri	>263	V	+	>176	V
P. pentosaceus	>250	VI	−	−	
S. aureus	>229	IV	+	>194	IV
S. epidermidis	>247	IV	+	>198	IV
S. haemolyticus	>238	IV	+	>202	IV
S. saprophyticus	>254	IV	+	73663370	IV
S. pneumoniae	>253	II	+	15901468	II
S. sanguinis	>266	II	+	125718462	II
S. thermophilum	>211	I	+	NM	

[a] Running number given as an identifier to each system in our data set (see Table S1 in the supplemental material).

[b] Group assignments according to our phylogenetic classification. NA, not assigned.

[c] The presence of a putative response regulator binding site in the region upstream of the ATPase gene of the transporter operon is indicated by "+," and lack of such a site is indicated by "−."

[d] The seven- to nine-digit numbers listed are the GI numbers of HKs identified in the genome as part of a candidate TCS for the regulation of orphan transporters. "−" indicates that no TCS with a BceS-like HK could be identified in the genome. NM, no match, i.e., a BceRS-like TCS associated with another Pep7E transporter is present in the genome but did not match the classification of the orphan transporter. Where it did match the classification of the transporter, its identifier in the data set is given preceded by ">."

[e] *E. faecalis*, *Enterococcus faecalis*; *G. thermodenitrificans*, *Geobacillus thermodenitrificans*; *L. acidophilus*, *Lactobacillus acidophilus*; *L. brevis*, *Lactobacillus brevis*; *L. casei*, *Lactobacillus casei*; *L. delbrueckii*, *Lactobacillus delbrueckii*; *L. gasseri*, *Lactobacillus gasseri*; *L. johnsonii*, *Lactobacillus johnsonii*; *L. plantarum*, *Lactobacillus plantarum*; *L. sakei*, *Lactobacillus sakei*; *L. innocua*, *Listeria innocua*; *L. welshimeri*, *Listeria welshimeri*; *P. pentosaceus*, *Pediococcus pentosaccus*; *S. epidermidis*, *Staphylococcus epidermidis*; *S. haemolyticus*, *Staphylococcus haemolyticus*; *S. saprophyticus*, *Staphylococcus saprophyticus*; *S. sanguinis*, *Streptococcus sanguinis*; *S. thermophilum*, *Symbiobacterium thermophilum*.

Firmicutes genomes are from those three orders) cannot be answered at this stage. The presence of multiple paralogous systems in one organism, together with a lack of genomic context conservation beyond the four genes under investigation in this study, suggests a diversification of the resistance modules through horizontal gene transfer and gene duplication. This is further supported by the limited correlation we found between phylogenetic groups and species distribution. Another notable finding was the uneven distribution of the number of systems per organism, as follows: species belonging to the *Bacillales* or *Clostridiales* often possessed many, in some cases up to six, Pep7E transporters, while members of the *Lactobacillales* generally contained only one or two. It therefore appears that resistance to antimicrobial peptides is of particular importance to bacteria that are predominantly found in the soil but only plays a minor role in the more specialized habitats (milk, skin, gut, etc.) of most lactic acid bacteria. Such an increased prevalence of antibiotic resistance mechanisms in the highly competitive soil environment has been demonstrated previously (16).

Coevolution. Analysis of the genetic loci of the ABC transporters showed a conserved cooccurrence of the encoding genes with operons encoding BceRS-like TCSs. Furthermore, qualitative and quantitative comparisons of the phylogeny of the permease and HK components of the resistance modules revealed a clear coevolutionary relationship between the two protein families. Coevolution of two protein families can be due to a number of reasons, such as participation of both proteins in the same physiological process, interaction of both proteins with the same ligand, or direct physical contact formation between the two proteins (43). In the case of the latter scenario, the evolutionary process can also be referred to as coadaptation, because changes in one protein partner will necessitate changes in the other partner to ensure their continued ability to interact (43). All three mechanisms could be envisaged to have led to the coevolution of BceB-like permeases and BceS-like HKs, based on their joined function in antimicrobial peptide resistance, potential interaction of both proteins with the substrate peptide, and protein-protein interaction between permease and HK. Because of the absolute requirement for the ABC transporter in stimulus detection by the TCS, such a direct interaction between both components is highly likely but still needs to be experimentally validated.

Substrate specificity. The classification of transport permeases into the eight phylogenetic groups presented here does not allow predictions regarding the function of uncharacterized systems, because we could not find any correlation between group assignment and substrate specificity. The same holds true for ECD sequence and substrate range. It may nevertheless be true that the ECD contains the substrate binding domain of the transporters and that the high degree of variability is required for adaptation to the large variety of substrates recognized by these modules. To date, the mode of substrate recognition by these transporters remains enigmatic, especially since a detailed study of inducer and resistance spectra of the Psd and Bce modules of *B. subtilis* showed their astonishing ability to distinguish between very similar substrates like actagardine and mersacidin while at the same time being able to recognize such structurally different substrates as nisin and enduracidin (48).

Regulatory networks and genomic rearrangements. Because permeases and HKs from one genetic locus are thought to be functionally linked and were found to generally fall into matching phylogenetic groups, we used our classification system to identify putatively corresponding TCSs for ABC transporters whose genes were not directly associated with a TCS operon. Such candidate systems, in which the HK of the TCS belonged to the same group as the transport permease, could be identified in about 50% of orphan transporters analyzed. While experimental validation is required for each TCS-transporter pair to prove their regulatory relationship, such evidence is

available in the literature for two of the systems included in our analysis.

In *Listeria monocytogenes*, one of the ABC transporters (Lmo1747-1746) is encoded in a genetic locus with the VirRS TCS (36), with both the permease and the HK VirS belonging to group V (Fig. 6B). It was recently shown that VirRS does not seem to regulate expression of the Lmo1747-1746 transporter (36), which explains the absence of a putative response regulator binding site upstream of Lmo1747. However, VirRS (Table 3, >174) is responsible for expression of a second orphan Pep7E-type ABC transporter, AnrAB (Table 3, >256) (12), which also belongs to group V and does possess a putative binding site in its promoter region (Fig. 6B). This association of a ABC transporter and TCS from separate genetic loci was thus correctly identified in our analysis. In further studies, it would be interesting to test if one or both of the two ABC transporters play a role in signaling, together with VirRS.

The second example is *S. aureus*, which possesses three Pep7E-type transporters, one from group II and two from group IV. The group II transporter (MW2543-2542) is associated with its own corresponding TCS, which was recently shown to be involved in nisin resistance and thus designated NsaRS (8). Of the group IV transporters, only one is encoded adjacent to a TCS (Fig. 6B). This is the GraRS(ApsRS)-VraFG module (Table 3, >194), where it has been shown that the GraRS TCS regulates expression of the VraFG transporter (34, 39). The second group IV transporter is VraDE (Table 3, >229), whose expression is partially controlled by GraRS (34), again matching our prediction. However, expression of *vraDE* is also dependent on the TCS NsaRS, as was shown recently in a study on bacitracin resistance of *S. aureus* (54). Mutants in *nsaRS* (named *bceRS* in the cited study), *mw2543-2542*, or *vraDE* all displayed increased sensitivity to bacitracin (54), thus indicating the existence of a more complex regulatory network: while it appears clear that NsaRS regulates the expression of both transporters (54), it has not been shown if both also mediate the actual resistance or if one transporter merely contributes to the signaling cascade. According to our classification, such a regulatory interaction with the HK would be possible only for the MW2543-2542 transporter, which belongs to the same phylogenetic group as NsaS (Fig. 6B).

A further example is the Spr0812-Spr0813 transporter from *Streptococcus pneumoniae* (Table 3, >253), for which we identified a TCS as the candidate regulator, based on coclustering of both permease and HK into group II. This is the same TCS identified previously, albeit without experimental evidence, as the most likely regulator of *spr0812-spr0813* expression (Fig. 6B) (5). Thus, the phylogenetic classification presented here provides a useful tool for the prediction of likely candidate systems for investigations into the regulatory mechanisms of such orphan transporters. The only group of permeases for which we could never identify a corresponding TCS was group VI. Since a complete response regulator binding site was also lacking for most, the regulation of transporters from this group remains unclear.

Functional link between HKs and transport permeases. The cooccurrence and coevolution of Pep7E transporters and the BceRS-like TCS described in this study lead us to hypothesize that a functional link always exists between these systems, in which they cooperate in both signaling and detoxification, as was shown for the bacitracin resistance modules of *B. subtilis* and *S. mutans* (42, 46). Based on their lack of an obvious input domain, BceS-like HKs have been termed intramembrane-sensing HKs and are thought to detect a stimulus at or within the cytoplasmic membrane (37). Even among the IM-HKs, the BceS-like proteins represent a kind of "minimal" system, because they do not even contain any cytoplasmic domains common to other HKs besides the DHp and catalytic domains required for autophosphorylation. Taken together with the observation that our database searches did not reveal any BceS homologs in genomes lacking a Pep7E transporter and only few transporters in genomes lacking a BceS homolog, we now propose that HKs of the BceS type cannot actually sense any stimulus directly but rather transfer the information received from their associated ABC transporter to their cognate response regulator.

An interesting scenario is presented in organisms containing multiple Pep7E transporters from the same phylogenetic group, encoded either in the same genetic locus or at different loci on the chromosome (Fig. 6). It is conceivable that in such situations, the two roles of the transporter have been split, with one transporter responsible for stimulus detection and the other for detoxification. Such an arrangement would explain the absence of putative regulator binding sites upstream of some transporters (e.g., *lmo1747-1746* in *L. monocytogenes* or transporters immediately downstream of the TCS in the tandem loci shown in Fig. 6A), as a transporter solely responsible for stimulus detection would not necessarily need to be induced in the presence of its substrate antimicrobial peptide.

In summary, the data presented here show the widespread distribution of unique and self-sufficient detoxification modules against antimicrobial peptides among *Firmicutes* bacteria and suggest a novel signaling and resistance mechanism involving formation of a sensory complex between transport permeases and HKs. To date, it has not been shown whether signaling is mediated by direct protein-protein interactions between permeases and HKs or whether the function of the transporter is merely the translocation of the substrate to the site at which it is directly sensed by the HK. However, initial results from bacterial two-hybrid assays in *Escherichia coli* suggest that the BceB permease and BceS HK of *B. subtilis* are indeed able to interact with each other (our unpublished results), lending support to the former hypothesis. While a number of key characteristics, such as the nature of such a sensory complex, the basis for substrate specificity, and the mechanism of both signal transduction and detoxification, will have to be addressed experimentally in the future, our study provides an ideal starting point for such investigations, especially regarding the elucidation of regulatory networks within and between these modules.

ACKNOWLEDGMENTS

We thank Ralf Zimmer for valuable input regarding calculations of correlation coefficients for multiple sequence alignments.

Work done in our laboratory was supported by grants-in-aid from the Fonds der Chemischen Industrie (to S.G.) and a grant from the Deutsche Forschungsgemeinschaft (to T.M.; grant MA2837/1-3).

REFERENCES

1. **Altschul, S. F., et al.** 1997. Gapped BLAST and PSI-BLAST: a new generation of protein database search programs. Nucleic Acids Res. **25:**3389–3402.

2. **Arthur, M., F. Depardieu, C. Molinas, P. Reynolds, and P. Courvalin.** 1995. The *vanZ* gene of Tn1546 from *Enterococcus faecium* BM4147 confers resistance to teicoplanin. Gene **154:**87–92.
3. **Bailey, T. L., and C. Elkan.** 1994. Fitting a mixture model by expectation maximization to discover motifs in biopolymers. Proc. Int. Conf. Intell. Syst. Mol. Biol. **2:**28–36.
4. **Baldauf, S. L.** 2003. Phylogeny for the faint of heart: a tutorial. Trends Genet. **19:**345–351.
5. **Becker, P., R. Hakenbeck, and B. Henrich.** 2009. An ABC transporter of *Streptococcus pneumoniae* involved in susceptibility to vancoresmycin and bacitracin. Antimicrob. Agents Chemother. **53:**2034–2041.
6. **Bernard, R., M. El Ghachi, D. Mengin-Lecreulx, M. Chippaux, and F. Denizot.** 2005. BcrC from *Bacillus subtilis* acts as an undecaprenyl pyrophosphate phosphatase in bacitracin resistance. J. Biol. Chem. **280:**28852–28857.
7. **Bernard, R., A. Guiseppi, M. Chippaux, M. Foglino, and F. Denizot.** 2007. Resistance to bacitracin in *Bacillus subtilis*: unexpected requirement of the BceAB ABC transporter in the control of expression of its own structural genes. J. Bacteriol. **189:**8636–8642.
8. **Blake, K. L., C. P. Randall, and A. J. O'Neill.** 2011. *In vitro* studies indicate a high resistance potential for the lantibiotic nisin in *Staphylococcus aureus* and define a genetic basis for nisin resistance. Antimicrob. Agents Chemother. **55:**2362–2368.
9. **Breukink, E., and B. de Kruijff.** 2006. Lipid II as a target for antibiotics. Nat. Rev. Drug Discov. **5:**321–332.
10. **Chevenet, F., C. Brun, A. L. Banuls, B. Jacq, and R. Christen.** 2006. TreeDyn: towards dynamic graphics and annotations for analyses of trees. BMC Bioinformatics **7:**439.
11. **Cole, C., J. D. Barber, and G. J. Barton.** 2008. The Jpred 3 secondary structure prediction server. Nucleic Acids Res. **36:**W197–W201.
12. **Collins, B., N. Curtis, P. D. Cotter, C. Hill, and R. P. Ross.** 2010. The ABC transporter, AnrAB, contributes to the innate resistance of *Listeria monocytogenes* to nisin, bacitracin and various beta-lactam antibiotics. Antimicrob. Agents Chemother. **54:**4416–4423.
13. **Cotter, P. D., C. Hill, and R. P. Ross.** 2005. Bacteriocins: developing innate immunity for food. Nat. Rev. Microbiol. **3:**777–788.
14. **Coumes-Florens, S., C. Brochier-Armanet, A. Guiseppi, F. Denizot, and M. Foglino.** 2011. A new highly conserved antibiotic sensing/resistance pathway in firmicutes involves an ABC transporter interplaying with a signal transduction system. PLoS One **6:**e15951.
15. **Crooks, G. E., G. Hon, J. M. Chandonia, and S. E. Brenner.** 2004. WebLogo: a sequence logo generator. Genome Res. **14:**1188–1190.
16. **D'Costa, V. M., K. M. McGrann, D. W. Hughes, and G. D. Wright.** 2006. Sampling the antibiotic resistome. Science **311:**374–377.
17. **de Been, M., M. J. Bart, T. Abee, R. J. Siezen, and C. Francke.** 2008. The identification of response regulator-specific binding sites reveals new roles of two-component systems in *Bacillus cereus* and closely related low-GC Grampositives. Environ. Microbiol. **10:**2796–2809.
18. **Dehal, P. S., et al.** 2010. MicrobesOnline: an integrated portal for comparative and functional genomics. Nucleic Acids Res. **38:**D396–D400.
19. **Dereeper, A., et al.** 2008. Phylogeny.fr: robust phylogenetic analysis for the non-specialist. Nucleic Acids Res. **36:**W465–W469.
20. **Detmers, F. J., F. C. Lanfermeijer, and B. Poolman.** 2001. Peptides and ATP binding cassette peptide transporters. Res. Microbiol. **152:**245–258.
21. **Draper, L. A., R. P. Ross, C. Hill, and P. D. Cotter.** 2008. Lantibiotic immunity. Curr. Protein Pept. Sci. **9:**39–49.
22. **Dubrac, S., P. Bisicchia, K. M. Devine, and T. Msadek.** 2008. A matter of life and death: cell wall homeostasis and the WalKR (YycGF) essential signal transduction pathway. Mol. Microbiol. **70:**1307–1322.
23. **Dutta, R., L. Qin, and M. Inouye.** 1999. Histidine kinases: diversity of domain organization. Mol. Microbiol. **34:**633–640.
24. **Felsenstein, J.** 1989. PHYLIP—Phylogeny Inference Package (version 3.2). Cladistics **5:**164–166.
25. **Gascuel, O.** 1997. BIONJ: an improved version of the NJ algorithm based on a simple model of sequence data. Mol. Biol. Evol. **14:**685–695.
26. **Goh, C.-S., A. A. Bogan, M. Joachimiak, D. Walther, and F. E. Cohen.** 2000. Co-evolution of proteins with their interaction partners. J. Mol. Biol. **299:** 283–293.
27. **Guder, A., I. Wiedemann, and H. G. Sahl.** 2000. Posttranslationally modified bacteriocins—the lantibiotics. Biopolymers **55:**62–73.
28. **Hall, T. A.** 1999. BioEdit: a user-friendly biological sequence alignment editor and analysis program for Windows 95/98/NT. Nucleic Acids Symp. Ser. **41:**95–98.
29. **Johnson, B. A., H. Anker, and F. L. Meleney.** 1945. Bacitracin: a new antibiotic produced by a member of the *B. subtilis* group. Science **102:**376–377.
30. **Joseph, P., G. Fichant, Y. Quentin, and F. Denizot.** 2002. Regulatory relationship of two-component and ABC transport systems and clustering of their genes in the *Bacillus/Clostridium* group, suggest a functional link between them. J. Mol. Microbiol. Biotechnol. **4:**503–513.
31. **Joseph, P., A. Guiseppi, A. Sorokin, and F. Denizot.** 2004. Characterization of the *Bacillus subtilis* YxdJ response regulator as the inducer of expression for the cognate ABC transporter YxdLM. Microbiology **150:**2609–2617.
32. **Kramer, N. E., S. A. van Hijum, J. Knol, J. Kok, and O. P. Kuipers.** 2006. Transcriptome analysis reveals mechanisms by which *Lactococcus lactis* acquires nisin resistance. Antimicrob. Agents Chemother. **50:**1753–1761.
33. **Letunic, I., T. Doerks, and P. Bork.** 2009. SMART 6: recent updates and new developments. Nucleic Acids Res. **37:**D229–D232.
34. **Li, M., et al.** 2007. The antimicrobial peptide-sensing system aps of *Staphylococcus aureus*. Mol. Microbiol. **66:**1136–1147.
35. **Majchrzykiewicz, J. A., O. P. Kuipers, and J. J. Bijlsma.** 2010. Generic and specific adaptive responses of *Streptococcus pneumoniae* to challenge with three distinct antimicrobial peptides, bacitracin, LL-37, and nisin. Antimicrob. Agents Chemother. **54:**440–451.
36. **Mandin, P., et al.** 2005. VirR, a response regulator critical for *Listeria monocytogenes* virulence. Mol. Microbiol. **57:**1367–1380.
37. **Mascher, T.** 2006. Intramembrane-sensing histidine kinases: a new family of cell envelope stress sensors in Firmicutes bacteria. FEMS Microbiol. Lett. **264:**133–144.
38. **Mascher, T., N. G. Margulis, T. Wang, R. W. Ye, and J. D. Helmann.** 2003. Cell wall stress responses in *Bacillus subtilis*: the regulatory network of the bacitracin stimulon. Mol. Microbiol. **50:**1591–1604.
39. **Meehl, M., S. Herbert, F. Götz, and A. Cheung.** 2007. Interaction of the GraRS two-component system with the VraFG ABC transporter to support vancomycin-intermediate resistance in *Staphylococcus aureus*. Antimicrob. Agents Chemother. **51:**2679–2689.
40. **Ohki, R., et al.** 2003. The BceRS two-component regulatory system induces expression of the bacitracin transporter, BceAB, in *Bacillus subtilis*. Mol. Microbiol. **49:**1135–1144.
41. **Ohki, R., et al.** 2003. A bacitracin-resistant *Bacillus subtilis* gene encodes a homologue of the membrane-spanning subunit of the *Bacillus licheniformis* ABC transporter. J. Bacteriol. **185:**51–59.
42. **Ouyang, J., X. L. Tian, J. Versey, A. Wishart, and Y. H. Li.** 2010. The BceABRS four-component system regulates the bacitracin-induced cell envelope stress response in *Streptococcus mutans*. Antimicrob. Agents Chemother. **54:**3895–3906.
43. **Pazos, F., and A. Valencia.** 2008. Protein co-evolution, co-adaptation and interactions. EMBO J. **27:**2648–2655.
44. **Pietiäinen, M., et al.** 2009. Transcriptome analysis of the responses of *Staphylococcus aureus* to antimicrobial peptides and characterization of the roles of *vraDE* and *vraSR* in antimicrobial resistance. BMC Genomics **10:**429.
45. **Pietiäinen, M., et al.** 2005. Cationic antimicrobial peptides elicit a complex stress response in *Bacillus subtilis* that involves ECF-type sigma factors and two-component signal transduction systems. Microbiology **151:**1577–1592.
46. **Rietkötter, E., D. Hoyer, and T. Mascher.** 2008. Bacitracin sensing in *Bacillus subtilis*. Mol. Microbiol. **68:**768–785.
47. **Saier, M. H., Jr., M. R. Yen, K. Noto, D. G. Tamang, and C. Elkan.** 2009. The Transporter Classification Database: recent advances. Nucleic Acids Res. **37:**D274–D278.
48. **Staroń, A., D. E. Finkeisen, and T. Mascher.** 2011. Peptide antibiotic sensing and detoxification modules of Bacillus subtilis. Antimicrob. Agents Chemother. **55:**515–525.
49. **Szurmant, H., T. Fukushima, and J. A. Hoch.** 2007. The essential YycFG two-component system of *Bacillus subtilis*. Methods Enzymol. **422:**396–417.
50. **Thompson, J. D., T. J. Gibson, and D. G. Higgins.** 2002. Multiple sequence alignment using ClustalW and ClustalX. Curr. Protoc. Bioinformatics **Chapter 2:**Unit 2.3.
51. **Tsuda, H., Y. Yamashita, Y. Shibata, Y. Nakano, and T. Koga.** 2002. Genes involved in bacitracin resistance in *Streptococcus mutans*. Antimicrob. Agents Chemother. **46:**3756–3764.
52. **Ulrich, L. E., and I. B. Zhulin.** 2010. The MiST2 database: a comprehensive genomics resource on microbial signal transduction. Nucleic Acids Res. **38:**D401–D407.
53. **Upton, M., J. R. Tagg, P. Wescombe, and H. F. Jenkinson.** 2001. Intra- and interspecies signaling between *Streptococcus salivarius* and *Streptococcus pyogenes* mediated by SalA and SalA1 lantibiotic peptides. J. Bacteriol. **183:** 3931–3938.
54. **Yoshida, Y., et al.** 2011. Bacitracin sensing and resistance in *Staphylococcus aureus*. FEMS Microbiol. Lett. **320:**33–39.